

# Dispersed materials for rechargeable lithium batteries: Reactive and non-reactive grinding

N. KOSOVA\*, E. DEVYATKINA

*Institute of Solid State Chemistry and Mechanochemistry SB RAS, Novosibirsk, Russia*  
E-mail: kosova@solid.nsc.ru

D. OSINTSEV

*Novosibirsk State University, Novosibirsk, Russia*

Reactive and non-reactive grinding has been used to prepare high dispersed lithium-transition metal cathode materials ( $\text{LiMn}_2\text{O}_4$ ,  $\text{LiCoO}_2$ ,  $\text{LiV}_3\text{O}_8$ ,  $\text{Li}_3\text{Fe}_2(\text{PO}_4)_3$ ,  $\text{LiTi}_2(\text{PO}_4)_3$ ) and inorganic solid state Li-ion electrolytes ( $\text{Li}_{1.3}\text{Al}_{0.3}\text{Ti}_{1.7}(\text{PO}_4)_3$ ) for rechargeable lithium batteries. Submicron particle size and the presence of cationic vacancies and cationic disordering positively influence electrochemical properties of as prepared cathodes, leading to larger practical capacity and stability upon intercalation-deintercalation of lithium ions. However, the advantages are observed only when the first electrochemical step is an insertion of  $\text{Li}^+$  ions (Li battery discharge). The conductivity of the  $\text{Li}_{1.3}\text{Al}_{0.3}\text{Ti}_{1.7}(\text{PO}_4)_3$  lithium ion electrolyte prepared by using MA was of 2–3 order of magnitude higher than that for nonactivated sample owing to the absence of non-conductive impurities and lower grain boundary resistance.

© 2004 Kluwer Academic Publishers

## 1. Introduction

Lithium and lithium-ion rechargeable batteries offer an operative voltage and energy density higher than those of the other rechargeable battery systems, and have various applications ranging from portable electronic devices to zero emission vehicles [1]. Rechargeable lithium batteries are based on the combination of lithium metal (or lithiated carbon) anode and a lithium—transition metal oxide intercalation cathode. 4 V intercalation compounds of layered and spinel structure, such as  $\text{LiCoO}_2$ ,  $\text{LiNiO}_2$ ,  $\text{LiMn}_2\text{O}_4$ , etc. and their derivatives, are most attractive cathodes in advanced lithium batteries. However, over the last few years, low cost iron-based compounds containing polyanions such as  $(\text{PO}_4)^{3-}$ ,  $(\text{SO}_4)^{2-}$  and  $(\text{AsO}_4)^{3-}$  are intensively investigated as potential cathode materials for large scale batteries [2].

The capacity of lithium batteries is limited mostly by the electrode materials. In this respect, much effort has been made to improve the performance of the electrode materials. For a long time, only well crystalline and micro-sized materials have been considered as good electrodes for lithium-ion cells. To increase practical capacity, to improve reversibility of electrodes and to provide the performance of Li insertion/extraction in kinetic regime, the preparation of high dispersed (submicron, nanocrystalline) and disordered materials is highlighted. The reason of positive influence of disordering of lithium-transition metal oxides on their electrochemical properties is in the larger stability of defect struc-

tures to the processes of intercalation of lithium ions. The presence of defects (especially, surface defects) in high dispersed cathode materials leads to smoother discharge curves, i.e. no formation of new phases accompanied by sharp structural changes occurs in comparison with well-crystalline homologue, and good reversibility is achieved. However, the advantages are observed only when the first electrochemical step is an insertion of  $\text{Li}^+$  ions (Li discharge battery).

To prepare high homogeneous, high dispersed and structurally disordered materials, low-temperature methods should be used, such as sol-gel or other solution techniques [3]. This can be also achieved by mechanical activation (MA) using non-reactive or reactive grinding. The main problem of applying MA to ceramic materials is contamination. To avoid this problem, different approaches are developing which are aimed to accelerate the exposure time. According to [4, 5], hydroxides or hydroxide-containing compounds appear to be more reactive in mechanochemical reactions compared to anhydrous oxides due to high reactivity of  $\text{OH}^-$  groups in the processes of proton and electron transfer and bond formation ('soft mechanochemical synthesis'). When using hydroxides, the level of mechanical loading decreases; providing softer activation conditions and lower level of contamination since the hardness of hydroxides is 3–4 times lower than for anhydrous oxides.

In this study, some results on preparation of high dispersed cathode and solid state electrolyte

\*Author to whom all correspondence should be addressed.

materials for rechargeable lithium batteries using MA are presented.

## 2. Reactive grinding

### 2.1. Lithium manganese spinel $\text{Li}_{1\pm x}\text{Mn}_2\text{O}_4$

Lithium manganese spinel  $\text{LiMn}_2\text{O}_4$  (space group Fd-3m) is one of the promising cathodes for rechargeable lithium batteries due to its lower cost and less toxicity as compared with  $\text{LiCoO}_2$ .  $\text{LiMn}_2\text{O}_4$  can cycle at 4 and 3 V ranges corresponding to the Li intercalation-deintercalation processes  $\text{LiMn}_2\text{O}_4 \leftrightarrow \lambda\text{-MnO}_2$  and  $\text{LiMn}_2\text{O}_4 \leftrightarrow \text{Li}_2\text{Mn}_2\text{O}_4$ , respectively. However, it is usually studied as 4 V cathode material since the capacity fades severely in the 3 V range when the average oxidation state of Mn falls below 3.5 due to the occurrence of Jahn-Teller distortion. Lithium insertion into  $\text{Li}_{1+x}\text{Mn}_2\text{O}_4$  ( $x > 0$ ) is, therefore, accompanied by the tetragonal phase formation. It has been shown that this can be overcome using materials prepared by low temperature methods provided a decrease of particle size and an increase of structural disorder and of the average oxidation state of manganese, the latter being more significant in the surface than in the bulk [6, 7]. Performing a systematic study by XPS, XAS,  $^7\text{Li}$  NMR analysis and electrochemical measurements for the  $\text{LiMn}_2\text{O}_4$  spinel oxides prepared at different temperatures, the authors [7] showed that the decreased sintering temperature modifies the surface properties in favor of a "grafting" of Li on the surface defects, which results in the reduction of surface  $\text{Mn}^{4+}$  into surface  $\text{Mn}^{3+}$  ions. It is well known that such surface  $\text{Mn}^{3+}$  ions would be easily disproportionated into  $\text{Mn}^{4+}$  and  $\text{Mn}^{2+}$  ions through contact with the electrolyte. In contrast to well crystallized spinel where  $\text{Mn}^{2+}$  ion is mostly dissolved into the electrolyte, the surface defects of low-temperature  $\text{LiMn}_2\text{O}_4$  can provide the stable tetrahedral sites for them [7].

In our studies, we performed the synthesis of  $\text{LiMn}_2\text{O}_4$  by reactive grinding in AGO-2 planetary mill starting from different lithium ( $\text{LiOH}$ ,  $\text{Li}_2\text{CO}_3$ ) and manganese ( $\text{MnO}$ ,  $\text{Mn}_2\text{O}_3$ ,  $\text{MnO}_2$ ) reagents [8–10]. It was shown that in the case of  $\text{MnO}_2$  and subsequent conditions of MA, the synthesis of lithium manganese spinel can be fully completed under MA at nearly room temperature compared to  $800^\circ\text{C}$  for ceramic method, or under subsequent short heat treatment of activated mixtures at moderate temperatures. The as prepared material is characterized by low crystallinity, high specific surface area (up to  $90\text{ m}^2/\text{g}$ ) with the average particle size of about 100–200 nm, and by decreased lattice constant evidencing, along with XPS data, an increased oxidation state of surface Mn ions (Fig. 1). According to IR and  $^7\text{Li}$  NMR spectroscopy, mechanochemically prepared  $\text{LiMn}_2\text{O}_4$  was distinguished by two kinds of disordering: cationic vacancies  $(\text{Li}_{1-x}\square_x)[(\text{Mn}^{4+}\text{Mn}^{3+})_{2-y}\square_y]\text{O}_4$  and cationic mixing  $\text{Li}_{\text{Td}} \leftrightarrow \text{Mn}_{\text{Oc}}$ .  $^7\text{Li}$  NMR spectrum of  $\text{LiMn}_2\text{O}_4$  was characterized by asymmetry. The resonance in the range  $>500$  ppm additional to the main peak of normal tetrahedral 8a Li site of the spinel structure at 470 ppm, was attributed to Li ions surrounded by increased number of neighboring oxygen atoms or Li ions near de-

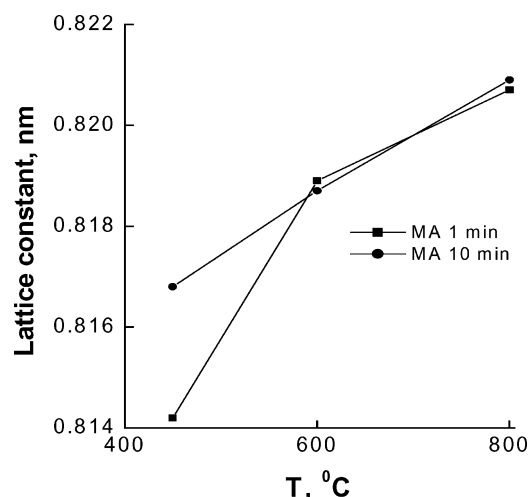


Figure 1 Lattice parameters of mechanochemically prepared  $\text{LiMn}_2\text{O}_4$  vs. temperature of subsequent heat treatment.

fects which might consist of vacancies. The width of the main peak was larger for mechanochemically prepared  $\text{LiMn}_2\text{O}_4$  than for ceramically prepared one and suggested a much broader distribution of  $\text{Mn}^{3+}$  and  $\text{Mn}^{4+}$  ions around tetrahedral  $\text{Li}^+$  in the former due to enhanced cationic mixing [10].

The as prepared samples were tested electrochemically over two ranges: 3.5–4.5 and 2.2–3.5 V in galvanostatic cell  $\text{Li}/\text{EC}$ ,  $\text{PC} + \text{LiPF}_6/\text{LiMn}_2\text{O}_4$ ,  $\text{C}$  [5]. It was established that the samples prepared by MA and subsequent heat treatment at  $400^\circ\text{C}$  are characterized by higher capacity ( $\sim 0.8$  Li) and better cycleability at 3 V range as compared with ceramically prepared samples though they show lower capacity when cycling at 4 V range as a result of low concentration of  $\text{Mn}^{3+}$  ions (Fig. 2). However, the capacity at 3 V range decreases upon increase of the temperature of heat treatment. In contrast, the reverse trend was observed for cycling at 4 V. This is associated with the increased oxidation state of Mn and the presence of structural disorder for the low-temperature samples, since by increase of the concentration of defects, it becomes easier for the material to accommodate the volume change associated with the intercalation process.

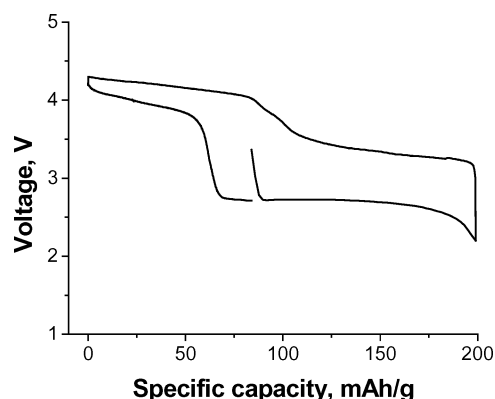


Figure 2 Galvanostatic discharge-charge curves for  $\text{LiMn}_2\text{O}_4$  (MA +  $450^\circ\text{C}$ ).

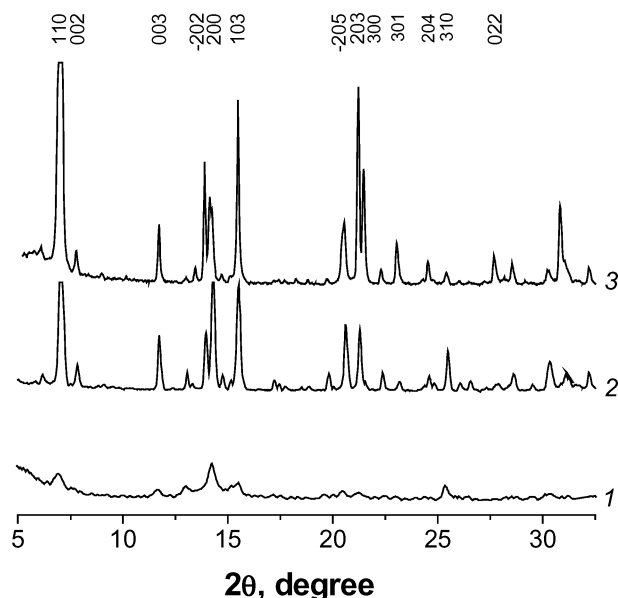


Figure 3 X-Ray patterns of  $\text{LiV}_3\text{O}_8$  prepared by mechanochemical synthesis (1); the same after heat treatment at  $400^\circ\text{C}$  (2) in comparison with  $\text{LiV}_3\text{O}_8$  prepared by melting at  $680^\circ\text{C}$  (3).

## 2.2. Lithium vanadium oxide $\text{Li}_{1+x}\text{V}_3\text{O}_8$

Last years, layered-structured  $\text{Li}_{1+x}\text{V}_3\text{O}_8$  (monoclinic space group  $\text{P2}_1/\text{m}$ ) is widely studied as a 3 V cathode material for rechargeable batteries because of its high capacity ( $\sim 200$  mAh/g), facile preparation and stability in air. It can reversibly insert up to 3.8 Li due to reduction of  $\text{V}^{5+}$  to  $\text{V}^{4+}$  and  $\text{V}^{3+}$ . The synthesis conditions of  $\text{Li}_{1+x}\text{V}_3\text{O}_8$  were shown to induce important differences in reversible capacity and cycling behavior. The improvement can be achieved both by expanding of interlayer spacing, which causes an increase in Li ion mobility, and by increased specific surface area [11, 12].

Mechanochemical synthesis of  $\text{Li}_{1+x}\text{V}_3\text{O}_8$  ( $x = 0.07 \div 0.1$ ) was realized in the mixtures of  $\text{LiOH}$  ( $\text{Li}_2\text{CO}_3$ ) and  $\text{V}_2\text{O}_5$ , both possessing a layered structure (Fig. 3). For electrochemical testing, the samples were heated up to  $200\text{--}400^\circ\text{C}$ . As prepared materials were characterized by residual amounts of  $\text{H}_2\text{O}$  and  $\text{CO}_2$  molecules in the interlayer spacing, thus increasing the latter and facilitating the process of lithium ions insertion. Specific surface area of as prepared material was about  $2\text{--}4$   $\text{m}^2/\text{g}$  [13]. It was shown that mechanochemical processing, along with solution technique, brings to higher capacity ( $>200$  mAh/g) and stable cycling behavior of the  $\text{Li}_{1+x}\text{V}_3\text{O}_8$  cathode material due to decreased particle size, lower degree of crystallinity, increased interlayer spacing and the absence of long-range order, reducing the pathway for lithium ions diffusion.

## 2.3. Lithium 3d-metal phosphates

Two extra Li ions can be theoretically inserted into rhombohedral  $\text{Li}_3\text{Fe}_2(\text{PO}_4)_3$  to form  $\text{Li}_5\text{Fe}_2(\text{PO}_4)_3$  at 2.8 V. The increase of the Li intercalation voltage for lithium 3d-metal compounds as compared with correspondent oxide systems is associated with strong bond

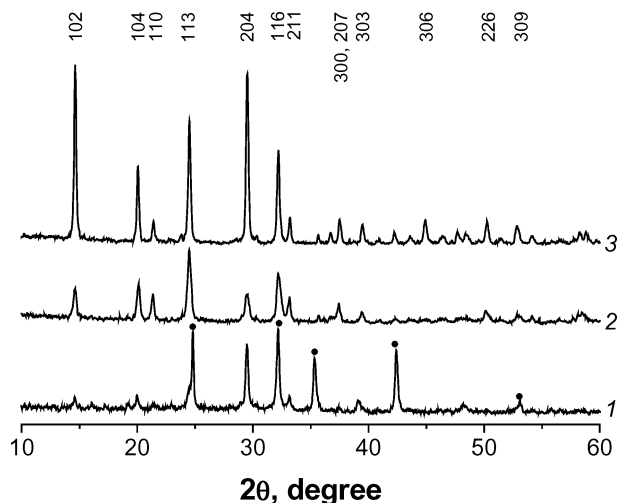


Figure 4 X-Ray patterns of  $\text{R-Li}_3\text{Fe}_2(\text{PO}_4)_3$  prepared via solid state mechanochemical (1, 2) and solution (3) ionic exchange with  $\text{LiNO}_3$ . 1—without washing, 2—after washing. ●— $\text{LiNO}_3$ .

covalency in polyanion X-O which stabilizes the antibonding  $\text{Me}^{n+1}/\text{Me}^n$  state through an Me-O-X inductive effect. The  $\text{Li}_3\text{Fe}_2(\text{PO}_4)_3$  discharge curves and the effective discharge capacity depend on the synthesis route. The authors [14] have found that after grinding, two plateaus at 2.8 and 2.65 V, corresponding to ca. 1.5–1.6 inserted Li ions, are observed instead of only one plateau at 2.8 V and ca. 1.1 inserted Li ions for untreated samples.

Rhombohedral  $\text{Li}_3\text{Fe}_2(\text{PO}_4)_3$  is usually prepared from monoclinic  $\text{Na}_3\text{Fe}_2(\text{PO}_4)_3$  by ionic exchange in a  $\text{LiNO}_3$  melt or in its concentrated aqueous solution. In the present study, to obtain monoclinic  $\text{Na}_3\text{Fe}_2(\text{PO}_4)_3$ , MA of the mixtures of  $\text{Fe}_2\text{O}_3$  and  $\text{NH}_4\text{H}_2\text{PO}_4$  with sodium hydroxides or carbonates was performed to accelerate solid state interaction under subsequent heat treatment at  $800^\circ\text{C}$ . Electrochemically active  $\text{R-Li}_3\text{Fe}_2(\text{PO}_4)_3$  was prepared by mechanochemical solid state ionic exchange reaction with as-prepared  $\text{Na}_3\text{Fe}_2(\text{PO}_4)_3$  using solid  $\text{LiNO}_3$  or  $\text{Li}_2\text{SO}_4$  (Fig. 4) whereas it did not occur in the mixture with  $\text{LiOH}$ . The products were washed with water to remove  $\text{NaNO}_3$  or  $\text{Na}_2\text{SO}_4$  and dried at  $100^\circ\text{C}$ . Chemical analysis shows that degree of ionic exchange reaches 65%. (Note, that monoclinic  $\text{Li}_3\text{Fe}_2(\text{PO}_4)_3$  does not transform into  $\text{R-Li}_3\text{Fe}_2(\text{PO}_4)_3$  under MA. Moreover, MA of monoclinic  $\text{Na}_3\text{Fe}_2(\text{PO}_4)_3$  hinders its ionic exchange with  $\text{LiNO}_3$  solution.) Three possible mechanism of mechanochemical ionic exchange can be proposed: (i) via formation of concentrated solutions; (ii) via contact melting, and (iii) via solid state reaction. Considering that the lithium salts were carefully dried before MA, and their melting points are drastically different ( $261$  and  $860^\circ\text{C}$ , respectively), the solid state mechanism is more evident. Note, that such exchange reactions can be realized in highly energetic activators only. The as prepared  $\text{R-Li}_{3-x}\text{Na}_x\text{Fe}_2(\text{PO}_4)_3$  was characterized by particle size of about  $50\text{--}100$  nm, i.e. by higher dispersion than that obtained in [14].

Recently, it has been shown that  $\text{LiTi}_2(\text{PO}_4)_3$  can also reversibly insert two lithium ions, operating on the  $\text{Ti}^{4+}/\text{Ti}^{3+}$  at 2.48 V vs.  $\text{Li}^+/\text{Li}$ , according to two-phase

mechanism between  $\text{LiTi}_2(\text{PO}_4)_3$  and  $\text{Li}_3\text{Ti}_2(\text{PO}_4)_3$ . The slightly lighter molecular weight of titanium as compared to iron induces a higher theoretical specific capacity than for iron isostructural materials: 138 mAh/g for  $\text{Li}_{1+x}\text{Ti}_2(\text{PO}_4)_3$  vs. 128 mAh/g for  $\text{Li}_{3+x}\text{Fe}_2(\text{PO}_4)_3$  [15]. Moreover, this compound can be used as inorganic solid state electrolyte for all solid state inorganic lithium batteries. We have shown that preliminary MA of the mixture of  $\text{TiO}_2$ ,  $\text{Li}_2\text{CO}_3$ , and  $\text{NH}_4\text{H}_2\text{PO}_4$  significantly decreases the temperature of subsequent heat treatment, providing higher homogeneity and decreased particle size of the final product, and higher Li ion conductivity (see below).

### 3. Non-reactive grinding

To get high dispersed materials, intensive non-reactive grinding is usually used. However, sometimes it is accompanied by decomposition processes. For instance, the authors [16–18] showed that after prolong grinding, a partial reduction and decomposition of  $\text{LiCoO}_2$  with the formation of  $\text{Co}_3\text{O}_4$  [16], or a phase that can be indexed in a cubic symmetry but whose exact stoichiometry is unknown [18], occur, thus worsening the electrochemical performance of the cathode material. Moreover, the prolong dispersion in ball and planetary mills leads to formation of aggregates which consist of fine particles. In further, friable and instable aggregates transform into more compact formations. This process is characterized by a decrease of specific surface area. To avoid decomposition and the aggregate formation, as well as to decrease the level of contamination, we activated  $\text{LiCoO}_2$  and  $\text{LiMn}_2\text{O}_4$  under mild conditions using so called 'grinding catalysts'. These compounds can be easily eliminated from cathode materials after MA.

According to chemical analysis, the amount of contamination in the ground materials appeared to be negligibly small. X-ray patterns show no traces of another phases. However, the reflections on X-ray patterns of activated samples become broader and less intensive evidencing the decrease of particle size and increased disorder. Table I shows the lattice parameters, crystallite size and microstrains of the ground  $\text{LiMn}_2\text{O}_4$  and  $\text{LiCoO}_2$  vs. grinding time pointing higher dispersion and disordering of the materials. IR spectra show no significant changes in the position of vibration bands, i.e. in the local structure of the ground materials (Fig. 5). However, for samples ground for 1 min, a strong increase of the intensity of bands corresponding to Co–O and Li–O bands for  $\text{LiCoO}_2$  and to lattice vibrations for  $\text{LiMn}_2\text{O}_4$  accompanied with their narrowing is observed while for the others the spectra become broader. After grinding for 10–20 min, one can see the additional weak bands at 1400–1500  $\text{cm}^{-1}$  in the spectra of the  $\text{LiCoO}_2$  samples indicating the presence of small amounts of adsorbed  $\text{CO}_3^{2-}$  groups. They are less intensive in the case of the ground  $\text{LiMn}_2\text{O}_4$ . Fig. 6 shows the EDRS spectra of the ground samples suggesting small changes in the electronic state for Mn ions contrary to drastic changes for Co ions upon grinding. For  $\text{LiMn}_2\text{O}_4$ , only small decrease of the bands' intensity of d-d transitions of Mn ions is observed at 10000–

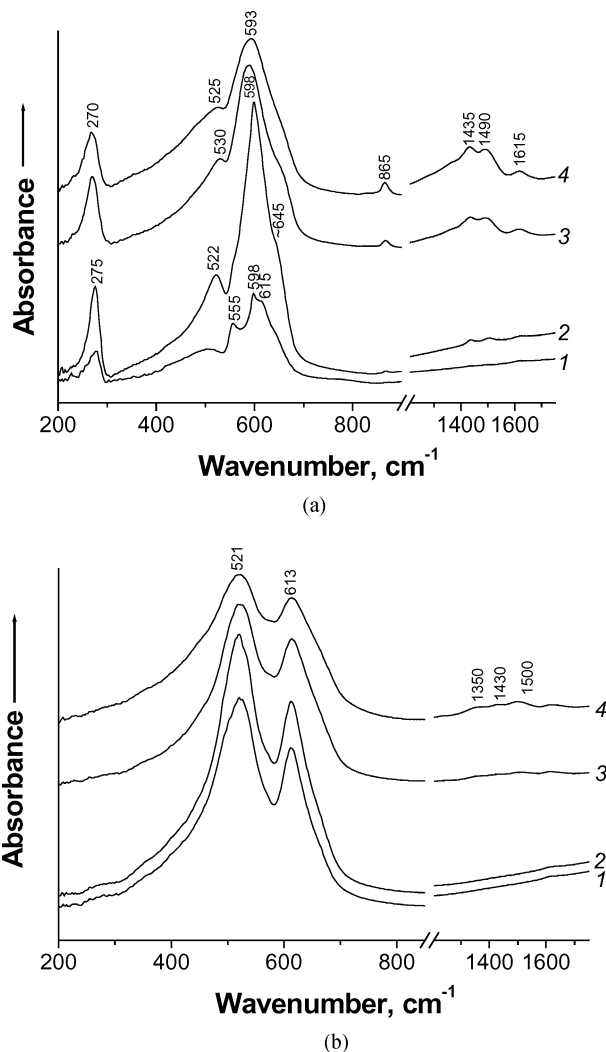


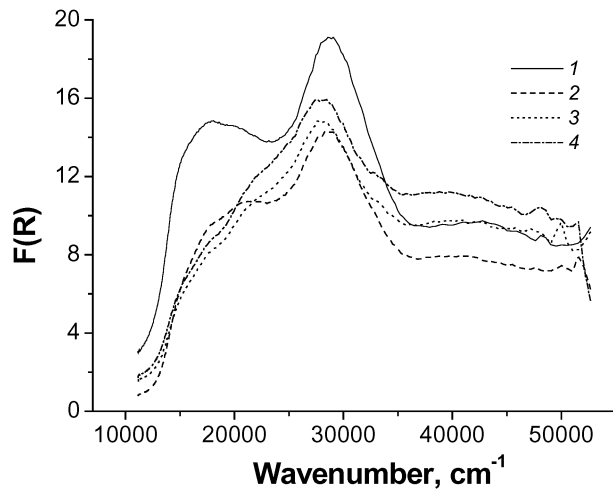
Figure 5 IR spectra of initial (1) and ground (2–4)  $\text{LiCoO}_2$  (a) and  $\text{LiMn}_2\text{O}_4$  (b): 2—1 min; 3—10 min; 4—20 min.

25000  $\text{cm}^{-1}$ , while their positions do not change drastically. In contrast, for  $\text{LiCoO}_2$ , the new absorption occurs at the 18000–22000  $\text{cm}^{-1}$  range, probably, corresponding to the appearance of  $\text{Co}^{2+}$  ions in the octahedral sites. The electrochemical study of the ground cathodes is under progress.

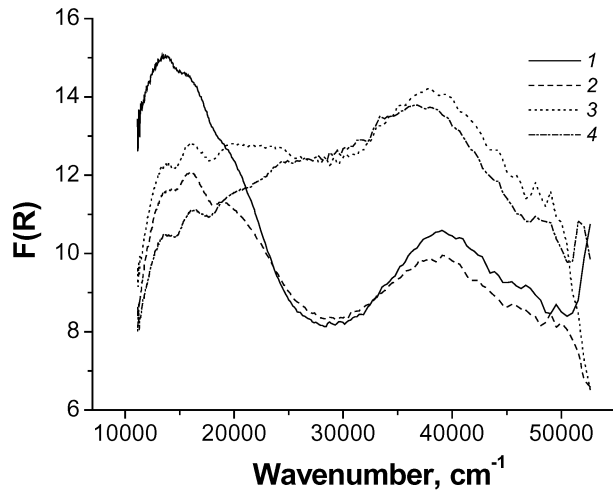
### 4. Solid state inorganic electrolytes

One of the new types of lithium batteries is solid state inorganic battery consisting of materials stable in air [19]. In order to prepare solid state inorganic batteries, it is necessary to choose solid state Li-ion conductor with high ionic conductivity and with linear thermal expansion coefficient close to that of electrode materials. Lanthanum lithium titanates with perovskite structure and doped lithium titanium phosphates with NASICON-like structure and with high ionic conductivity (ca.  $10^{-3}$ – $10^{-4}$   $\text{S} \cdot \text{cm}^{-1}$  at room temperature) appeared to be rather perspective solid state electrolytes.

Unlike other NASICON compounds, undoped  $\text{LiTi}_2(\text{PO}_4)_3$  has poor ionic conductivity (ca.  $10^{-6}$ – $10^{-8}$   $\text{S} \cdot \text{cm}^{-1}$ ). However, by substitution of trivalent cations for  $\text{Ti}^{4+}$  cations in the octahedral sites of  $\text{LiTi}_2(\text{PO}_4)_3$ , Li ion conductivity is significantly



(a)



(b)

Figure 6 EDRS spectra of initial (1) and ground (2–4)  $\text{LiCoO}_2$  (a) and  $\text{LiMn}_2\text{O}_4$  (b): 2—1 min; 3—10 min; 4—20 min.

improved. Al-substituted compound with nominal composition  $\text{Li}_{1.3}\text{Al}_{0.3}\text{Ti}_{1.7}(\text{PO}_4)_3$  was shown to have the optimum Li ionic conductivity [20].

To prepare  $\text{Li}_{1.3}\text{Al}_{0.3}\text{Ti}_{1.7}(\text{PO}_4)_3$ , a mixture of  $\text{TiO}_2$ ,  $\text{Li}_2\text{CO}_3$ ,  $\text{Al}(\text{OH})_3$  and  $\text{NH}_4\text{H}_2\text{PO}_4$  was mechanically activated that allowed obtaining more dispersed and homogeneous final product at decreased temperature ( $800^\circ\text{C}$  instead of  $1000^\circ\text{C}$ ). The value of conductivity of thus prepared samples was of 2 order of magnitude higher than that for nonactivated samples owing to the absence of impurities and, probably, to lower grain boundary resistance (Fig. 7). For the latter, the formation of different non-conductive impurities (such as  $\text{TiO}_2$ ,  $\text{TiP}_2\text{O}_7$ ,  $\text{AlPO}_4$ ) was observed at this temperature worsening their ionic conductivity. The activation energy for mechanochemically prepared samples slightly decreases from 0.263 to 0.205 eV for  $\text{LiTi}_2(\text{PO}_4)_3$  and from 0.191 to 0.147 eV for  $\text{Li}_{1.3}\text{Al}_{0.3}\text{Ti}_{1.7}(\text{PO}_4)_3$ . Non-reactive grinding of  $\text{LiTi}_2(\text{PO}_4)_3$  and  $\text{Li}_{1.3}\text{Al}_{0.3}\text{Ti}_{1.7}(\text{PO}_4)_3$  as well as reactive grinding also leads to enhanced Li ion conductivity (Fig. 8). It should be noted that this is associated with the increased grain boundary conductivity whereas bulk conductivity remains practically unchanged.

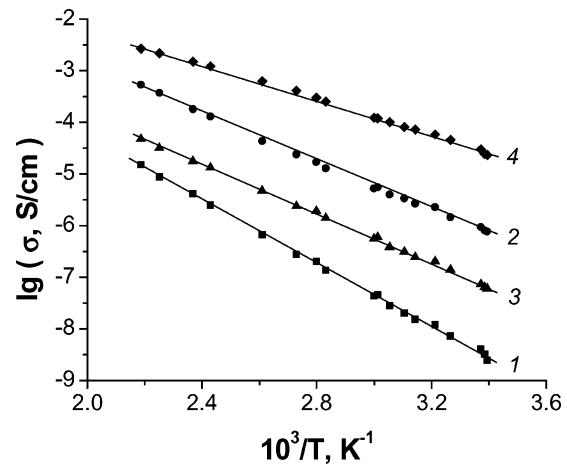
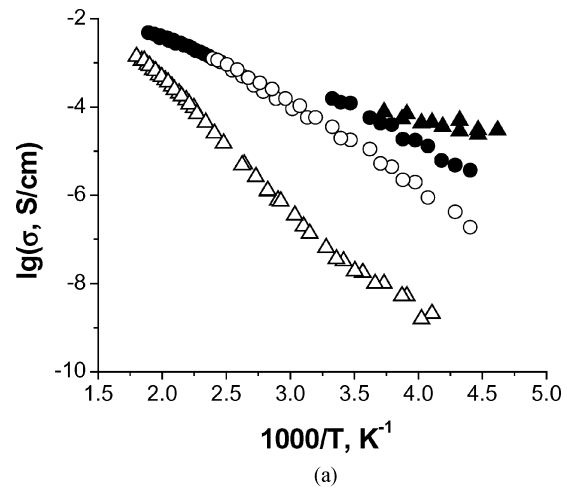
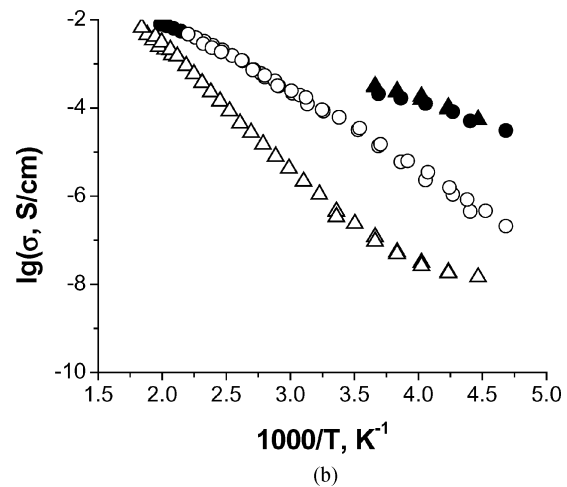


Figure 7 Arrhenius dependencies for conductivity of  $\text{LiTi}_2(\text{PO}_4)_3$  (1, 2) and  $\text{Li}_{1.3}\text{Al}_{0.3}\text{Ti}_{1.7}(\text{PO}_4)_3$  (3, 4): 1, 3—prepared without MA; 2, 4—with MA.



(a)



(b)

Figure 8 Bulk and grain boundary conductivity of ground and non-ground  $\text{LiTi}_2(\text{PO}_4)_3$  (a) and  $\text{Li}_{1.3}\text{Al}_{0.3}\text{Ti}_{1.7}(\text{PO}_4)_3$  (b). Triangles—non-ground, circles—ground, filled—bulk conductivity, open—grain boundary conductivity.

## 5. Conclusion

Thus, it has been demonstrated that MA can be successfully used for preparation of the lithium-transition metal cathode materials for rechargeable lithium batteries. They are characterized by high dispersion and structural disordering. Submicron particle size, the

presence of cationic vacancies and cationic disordering, and the increased interlayer spacing positively influence their electrochemical properties leading to larger practical capacity and stability upon intercalation-deintercalation of lithium ions. However, the advantages are mostly observed only when the first electrochemical step is an insertion of Li<sup>+</sup> ions (Li discharge battery). Lithium titanium phosphates prepared by reactive as well as by non-reactive grinding show enhanced Li ion conductivity.

### Acknowledgements

The authors would like to thank G. Tomilova, N. Uvarov, I. Asanov, S. Kozlova, V. Anufrienko, A. Badalyan for their contribution to this study.

### References

1. B. SCROSATI, *Electrochim. Acta* **45** (2000) 2461.
2. A. K. PADHI, K. S. NANJUNDASWAMY and J. B. GOODENOUGH, *J. Electrochem. Soc.* **144** (1997) 1188.
3. C. W. KWON, S. J. HWANG, A. POQUET, N. TREUIL, G. CAMPET, J. PORTIER and J. H. CHOY, in "New Trends in Intercalation Compounds for Energy Storage", edited by C. Julien *et al.* (Kluwer Academic Publishers, Dordrecht, 2002) p. 439.
4. E. AVVAKUMOV, M. SENNA and N. KOSOVA, "Soft Mechanochemical Synthesis: A Basis for New Chemical Technologies" (Kluwer Academic Publishers, Boston, 2001).
5. N. KOSOVA and E. DEVYATKINA, *Ann. Chim. Sci. Mat.* **27** (2002) 77.
6. P. BARBOUX, J. M. TARASCON and F. K. SHOKOHI, *J. Solid State Chem.* **94** (1991) 185.
7. N. TREUIL, C. LABRUGERE, M. MENETRIER, J. PORTIER, G. CAMPET, A. DESHAYES, J.-C. FRISON, S.-J. HWANG, S.-W. SONG and J.-H. CHOY, *J. Phys. Chem. B* **103** (1999) 2100.
8. N. V. KOSOVA, N. F. UVAROV, E. T. DEVYATKINA and E. G. AVVAKUMOV, *Solid State Ionics* **135** (2000) 107.
9. N. V. KOSOVA, I. P. ASANOV, E. T. DEVYATKINA and E. G. AVVAKUMOV, *Solid State Chem.* **146** (1999) 184.
10. N. V. KOSOVA, E. T. DEVYATKINA and S. G. KOZLOVA, *J. Power Sources* **97/98** (2001) 406.
11. V. MANEV, A. MOMCHILOV, A. NASSALEVSKA, G. PISTOIA and M. PASQUALI, *ibid.* **54** (1995) 501.
12. D. GUYOMARD, in "New Trends in Electrochemical Technology: Energy Storage Systems in Electronics", edited by T. Osaka and M. Datta (Gordon & Breach Publ., Philadelphia, 2000) Ch. 9, p. 253.
13. N. V. KOSOVA, S. V. VOSEL, V. F. ANUFRIENKO, N. T. VASENIN and E. T. DEVYATKINA, *J. Solid State Chem.* **160** (2001) 444.
14. A. S. ANDERSSON, B. KALSKA, P. EYOB, D. AERNOU, L. HÄGGSTRÖM and J. O. THOMAS, *Solid State Ionics* **140** (2001) 63.
15. S. PATOUX and C. MASQUELIER, in Proceedings of the 11 International Meeting on Lithium Batteries, edited by F. McLarnon (Monterey, California, June 2002).
16. J. M. FERNANDEZ-RODRIGUEZ, J. MORALES and J. L. TIRADO, *React. Solids* **4** (1987) 163.
17. M. N. OBROVAC, O. MAO and J. R. DAHN, *Solid State Ionics* **112** (1998) 9.
18. N. V. KOSOVA, V. F. ANUFRIENKO, T. V. LARINA, A. ROUGIER, L. AYMARD and J. M. TARASCON, *J. Solid State Chem.* **165** (2002) 56.
19. T. BROUSSE, P. FRAGNAUD, R. MARCHAND, D. M. SCHLEICH, O. BOHNKE and K. WEST, *J. Power Sources* **68** (1997) 412.
20. H. AONO, E. SUGIMOTO, Y. SADAOKA, N. IMANAKA and G. ADACHI, *J. Electrochem. Soc.* **136** (1989) 590.

Received 11 September 2003  
and accepted 27 February 2004